npj | quantum materials

www.nature.com/npjquantmats

ARTICLE OPEN

Check for updates

Quantum critical Eliashberg theory, the Sachdev-Ye-Kitaev superconductor and their holographic duals

Gian-Andrea Inkof[1]✉, Koenraad Schalm[2]✉ and Jörg Schmalian[1,3]✉

Superconductivity is abundant near quantum critical points, where fluctuations suppress the formation of Fermi liquid quasiparticles and the BCS theory no longer applies. Two very distinct approaches have been developed to address this issue: quantum-critical Eliashberg theory and holographic superconductivity. The former includes a strongly retarded pairing interaction of ill-defined fermions, the latter is rooted in the duality of quantum field theory and gravity theory. We demonstrate that both are different perspectives of the same theory. We derive holographic superconductivity in form of a gravity theory with emergent space-time from a quantum many-body Hamiltonian—the Yukawa Sachdev-Ye-Kitaev model—where the Eliashberg formalism is exact. Exploiting the power of holography, we then determine the dynamic pairing susceptibility of the model. Our holographic map comes with the potential to use quantum gravity corrections to go beyond the Eliashberg regime.

npj Quantum Materials (2022)7:56 ; https://doi.org/10.1038/s41535-022-00460-8

INTRODUCTION

Superconductivity is the natural ground state of a clean metal with Fermi liquid properties. A cornerstone of paired-electron superconductivity in Fermi liquids is Eliashberg theory[1,2], which extends BCS theory by accounting for the dynamics of soft boson quanta that mediate the electron-electron interaction[3]. Experimentally, superconductivity is particularly abundant near quantum critical points[4–6]; yet here electrons no longer form a Fermi liquid and the Cooper instability paradigm does not apply. Indeed, repeating Cooper's analysis for a non-Fermi liquid but with instantaneous pairing interaction[7] suggests, at first glance, that superconductivity should rather be the exception than the rule[7–9]. Important progress was made by realizing that dynamical retardation effects —naturally present in the Eliashberg formalism—are crucial in critical systems[10–16]. Examples are gauge-field induced composite fermion pairing[17,18], color magnetic interaction in high-density quark matter[12,19], superconductivity due to magnetic[10,11,20] or Ising nematic[18,21] quantum critical fluctuations, or pairing in $U(1)$ and Z_2 spin-liquid states[18]. The justification of the quantum-critical Eliashberg theory is in many of these cases far from clear. While it is believed to capture the most relevant dynamics and the scaling properties[22,23] a different perspective of its validity is clearly desirable.

A tremendous amount of insight into quantum critical systems has been gained from a fundamentally different perspective given by the holographic dual formulation in terms of a higher-dimensional Anti-de Sitter (AdS) space[24–26]. This also extends to superconductivity. The holographic superconductor[27,28] can consistently describe order-parameter condensation in strongly coupled theories without quasiparticles and naturally encapsulates quantum critical points (QCPs) in addition to thermal transitions. Also here, these results are often pushed beyond the matrix large-N theories for which holography is formally justified. This should capture the most relevant dynamics, even though reliable quantitative information is, in essence, limited to systems where additional symmetries constrain the holographic model enough, e.g. the canonical example of $\mathcal{N}=4$ super Yang–Mills[29], or, as of relevance here, the (0+1)-dimensional model of Sachdev-Ye-Kitaev (SYK)[30–32].

In this article, we show how the mutually complementary regimes of quantum critical Eliashberg theory and holographic superconductivity actually overlap and are, in fact, different perspectives of the same identical physics. We obtain an explicit transformation of the Yukawa-SYK theory that makes the gravitational character, contained in the critical normal state, explicit for superconducting instabilities. In this sense, we derive holographic superconductivity in form of a gravity theory with emergent space-time from a quantum many-body Hamiltonian where the Eliashberg formalism is exact. Our result fleshes out early indications that order parameter susceptibilities can be matched this way[33], and this map also gives an explicit physical meaning of the additional holographic coordinate in terms of the two time variables that occur in pair correlation functions. We focus on the quantum-critical transition to superconductivity in SYK-like models. This model describes a $0+1$-dimensional quantum system and can obviously only serve as a toy model for realistic systems. However, there is evidence that our approach is relevant for finite-dimensional compressible quantum critical metals: systems with negligible momentum dependence of the self energy[10–16] yield an Eliashberg equation that is identical to ours and, as we will see, that can be rewritten as a Klein–Gordon equation in AdS_2. Furthermore, the Yukawa-SYK model discussed in this paper was recently extended to describe critical Fermi surfaces in two dimensions[34]. Generalizing our holographic map to this model we expect a description in $AdS_2 \otimes \mathbb{R}_2$. Hence, the quantum critical Eliashberg approach of refs. [10–16] should be applicable whenever the low-energy holographic description has an AdS_2 sector, and, vice versa, that the holographic AdS_2 description can be used in systems where the quantum critical Eliashberg equations apply.

In the normal state, the SYK model is described by a low-energy effective action, the so-called Schwarzian theory, that can also be

[1]Institute for Theory of Condensed Matter, Karlsruhe Institute of Technology, 76131 Karlsruhe, Germany. [2]Instituut-Lorentz, Δ-ITP, Universiteit Leiden, P.O. Box 9506, 2300 RA, Leiden, The Netherlands. [3]Institute for Quantum Materials and Technologies, Karlsruhe Institute of Technology, Karlsruhe 76021, Germany. ✉email: gian.inkof@kit.edu; kschalm@lorentz.leidenuniv.nl; joerg.schmalian@kit.edu

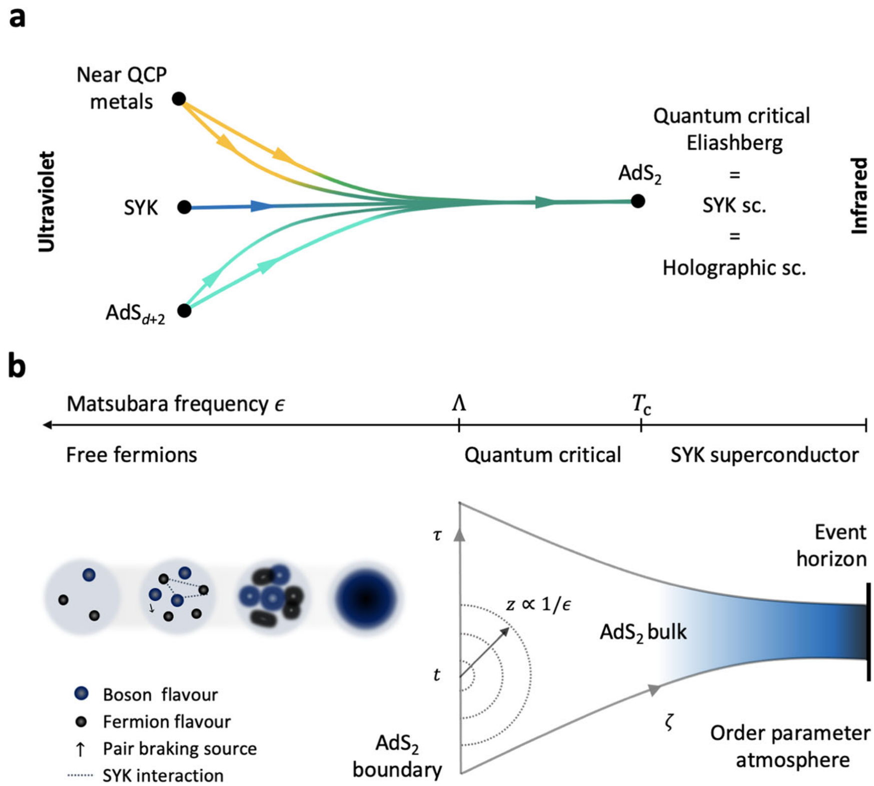

Fig. 1 The emergence of the dual holographic theory from the SYK superconductor. a The semi-universal low-energy holographic action equal to quantum critical Eliashberg theory describing the IR of holographic superconductors (AdS$_{d+2}$), SYK superconductors, and metals near quantum critical points. **b** Below the UV scale Λ, a strongly coupled quantum-critical fluid forms out of interacting fermions and bosons. Below this scale, the fluctuating order parameter becomes a scalar field with emergent AdS$_2$ gravity and forms an atmosphere around a black hole event horizon. The frequency ϵ of the relative time $\tau_1 - \tau_2$ and the absolute time $t = (\tau_1 + \tau_2)/2$ of SYK pairing fields $F(\tau_1, \tau_2) = \frac{1}{N}\sum_{i=1}^{N} c_{i\uparrow}(\tau_1)c_{i\downarrow}(\tau_2)$ determine the set of geodesic half circles that span the anti-de Sitter space (τ, ζ) on the gravity side.

derived from two-dimensional gravity with a scalar field (the dilaton)[35–38], where the same pattern of breaking of the conformal symmetry occurs. In fact, the structure of the Schwarzian action can be guessed with considerations of conformal symmetry alone—see refs. [36,39] for cases where the low-energy action is dominated by non-local terms. In stark contrast, our map between SYK-Eliashberg theory and holography clearly cannot be derived using conformal symmetry alone: the presence of an explicit scale, the critical temperature T_c, breaks scale-invariance, and the dynamical equation of order parameter formation is sensitive to certain details of the system. Instead, the SYK-Eliashberg dynamics and its holographic equivalent describe the semi-universal RG-flow; semi-universal in the sense that it is grounded in a universal quantum critical SYK superconducting transition in the infrared (IR) from which it inherits certain universal scaling properties, but may have different microscopic, ultraviolet (UV) origins. This is sketched in Fig. 1.

Using this map as an anchor, we exploit the power of holography to investigate the previously unknown dynamical pairing response of the SYK superconductor. This can be seen as an extension of the mapping of DC transport in Wilson–Fisher-type QCPs to holography, and using this map to predict finite-frequency responses near criticality[40].

RESULTS

SYK-Eliashberg

The explicit example of Eliashberg's theory for a tractable strongly coupled quantum critical point we shall focus on is the SYK superconductor constructed in ref. [41] (see also refs. [42–47]). This is a generalization of the complex SYK model with N charge-q, spin-1/2 fermions $c_{i\sigma}$, and four-fermion interactions to a more generic Yukawa interaction with M soft bosons ϕ_k

$$\begin{aligned} H = & -\mu \sum_{i=1,\sigma=\uparrow\downarrow}^{N} c_{i\sigma}^{\dagger} c_{i\sigma} + \frac{1}{2}\sum_{k=1}^{M}\left(\pi_k^2 + \omega_0^2 \phi_k^2\right) \\ & + \frac{1}{N}\sum_{ijk\sigma}^{M,N}\left(g_{ij,k} + g_{ji,k}^{*}\right) c_{i\sigma}^{\dagger} c_{j\sigma}\phi_k . \end{aligned} \tag{1}$$

In essence, it encodes fermions coupled to a large number of Einstein phonons at a common frequency ω_0 in the strong coupling limit.

Disorder averaging over the interactions $g_{ij,k}$ around a zero mean can induce superconductivity in states without quasiparticles if $g_{ij,k} = (g_k)_{ij}$ are sampled from the Gaussian Orthogonal Ensemble rather than the Gaussian Unitary Ensemble with variance $\bar{g}^2$. Interpolating between the two ensembles by introducing a pair-breaking parameter $0 \le \alpha \le 1$ further allows to continuously vary the superconducting transition temperature T_c and tune it to vanish at a quantum critical point[45]. α is defined in Eq. (19) of the methods section. These results follow after a rewriting of the path-integral in terms of bilocal propagator fields $G(\tau_1, \tau_2) = \frac{1}{N}\sum_{i=1}^{N} c_{i\sigma}^{\dagger}(\tau_1)c_{i\sigma}(\tau_2)$ and $F(\tau_1, \tau_2) = \frac{1}{N}\sum_{i=1}^{N} c_{i\uparrow}(\tau_1)c_{i\downarrow}(\tau_2)$ that correspond at the large-N saddle point to the normal and anomalous Green's function of the Nambu-Eliashberg formalism[48]. Both have conjugate fields $\Sigma(\tau_1, \tau_2)$ and $\Phi(\tau_1, \tau_2)$ that play the role of self energies. The (Euclidean) action of the analysis is rather lengthy and can be found in the Methods section. In the large N, M limit with M/N fixed, the equations of motion are recognized as strongly coupled Eliashberg equations[41–45].

In the normal state $F(\tau_1, \tau_2) = \Phi(\tau_1, \tau_2) = 0$, and the theory flows to an SYK critical state defined by the time-translation invariant scaling dynamics with fermion and boson propagators

$$\begin{aligned} G_{\rm n}(\tau_1-\tau_2) &= b_g \frac{\tanh(\pi q\mathcal{E})+\mathrm{sign}(\tau_1-\tau_2)}{|\tau_1-\tau_2|^{\frac{1+\gamma}{2}}}, \\ D_{\rm n}(\tau_1-\tau_2) &= b_d \frac{1}{|\tau_1-\tau_2|^{1-\gamma}}. \end{aligned} \quad (2)$$

The exponent $0 < \gamma < 1$ can be tuned by varying the ratio M/N and the charge density n via Eq. (28) of the methods section. In the SYK literature, one frequently uses $\Delta = (1+\gamma)/4$ instead of γ. The spectral asymmetry parameter $\mathcal{E}$ can be directly related to the particle density $n = \langle c^{\dagger}_{i\sigma} c_{i\sigma}\rangle$ via a generalized Luttinger theorem[49,50], where $\mathcal{E}(n = 1/2) = 0$. It is also linked to the density dependence of the zero-point entropy[51] $2\pi\mathcal{E} = \frac{\partial S_0}{\partial n}$. While the two coefficients $b_{g,d}$ depend on details of the UV behavior, the important combination $\mu_\gamma \equiv \bar{g}^2 b_d b_g^2 = \frac{\gamma}{4\pi}\cosh^2(\pi q\mathcal{E})\tan(\pi\gamma/2)$ is dimensionless and universal. Thus, the normal state of the Hamiltonian (1) is a strongly coupled, quantum-critical fluid made of interacting fermions and bosons.

In the superconducting state in the vicinity of the phase transition, F and Φ remain small. Confining ourselves to Gaussian fluctuations in the disordered phase, we may then expand the action to second-order and integrate out Φ. As discussed in the Methods section, this yields the leading contributions of superconducting fluctuations to the SYK action:

$$\begin{aligned} S^{(\rm sc)}/N = &\int_{\omega,\epsilon} \frac{F^{\dagger}(\omega,\epsilon)F(\omega,\epsilon)}{\Pi_{\rm n}(\omega,\epsilon)} \\ &- \frac{\bar{g}^2\lambda_p}{2}\int_{\omega,\epsilon,\epsilon'} F^{\dagger}(\omega,\epsilon) D_{\rm n}(\epsilon-\epsilon')F(\omega,\epsilon'). \end{aligned} \quad (3)$$

Here, we Fourier transformed $F(\tau_1, \tau_2)$ with regards to the relative time $\tau_1 - \tau_2$, with frequency ϵ, and absolute time $t = (\tau_1 + \tau_2)/2$, with frequency ω, respectively. $\int_\omega \cdots = T\sum_n \cdots$ stands for the sum over Matsubara frequencies. $\lambda_p = (1-\alpha)M/N$ modifies the coupling constant in the pairing channel and depends on the pair-breaking strength α. The first term in Eq. (3) is determined by the particle-particle response function $\Pi_{\rm n}(\omega,\epsilon) = G_{\rm n}\left(\frac{\omega}{2}-\epsilon\right)G_{\rm n}\left(\epsilon+\frac{\omega}{2}\right)$ of the critical normal state. The second term contains the singular pairing interaction with the boson propagator $D_{\rm n}(\epsilon)$.

Eq. (3) is then the IR effective action for the dynamic order parameter $F(\omega)_\epsilon = F(\omega, \epsilon)$ parametrized by a microscopic energy ϵ. In the dynamics of BCS theory, the ϵ-dependence is neglected. The Eliashberg dynamics makes clear that ϵ is the relative energy of the fermions, and therefore representative of the characteristic energy at which the system is probed. One can indeed think of it as an RG scale, as our mapping to a holographic model will make clear.

From Eliashberg to holography

Next, we establish a holographic map based on the effective action (3). We first consider the case $T = \mu = 0$. It is convenient to only perform the Fourier transform $F(t,\epsilon)$ with respect to the relative time and keep the absolute time t. From the Pauli principle for singlet, even-frequency pairing follows that $F(t,\epsilon)$ does not depend on the sign of ϵ. This allows us to introduce the scalar Bose field

$$\tilde{\psi}(t,z) = c_0 z^{\frac{\gamma-1}{2}} F(t, c/z), \quad (4)$$

with $z = c|\epsilon|^{-1}$ and positive coefficients c and c_0. This relation is in general non-local in z but takes the local form of Eq. (4) in the limit of low energy—see Methods section for details. Performing an inverse Radon transform $\tilde{\psi}(t,z) \to \psi(\tau,\zeta)$—a necessity pointed out in[35,52]—that maps pairs of points (t, z) to a point (τ, ζ) on an AdS_2 geodesic, at low energy it then follows that the SYK theory takes the form

$$S^{(\rm sc)}/N = \int d\tau d\zeta \left(\frac{m^2}{\zeta^2}|\psi|^2 + |\partial_\tau\psi|^2 + |\partial_\zeta\psi|^2\right). \quad (5)$$

This is the action of a holographic superconductor in AdS_2 with mass m and with Euclidean signature:

$$ds^2 = g_{ab}dx^a dx^b = \frac{1}{\zeta^2}\left(d\tau^2 + d\zeta^2\right). \quad (6)$$

This derivation of a holographic map between strongly coupled SYK-Eliashberg theory and its equivalent AdS-description, with the extra, radial direction ζ encoding the RG scale, is the central result of this paper. The weak-to-strong coupling duality emerges through an explicit map since we start out from an exact strong-coupling normal state solution. In the methods section we give further details on the derivation of Eq. (5), and give explicit expressions for the constants c and c_0 as well as the mass m in terms of the parameters of the Hamiltonian (1). The time derivative in Eq. (5) originates from the first term in Eq. (3) and is due to the ω-dependence of the particle-particle bubble $\Pi_{\rm n}(\omega, \epsilon)$. The kinetic term in the radial direction of the holographic bulk is due to the singular pairing interaction $D_{\rm n}(\epsilon)$. Both terms contribute to the AdS_2 mass m. The anomalous power-law dependence $\Pi_{\rm n}(0, \epsilon) \sim |\epsilon|^{\gamma-1}$ yields a positive contribution $m^2_{(1)} > 0$, which reflects the absence of a naive Cooper instability in critical non-Fermi liquids[7,8]. However, the singular pairing interaction $D_{\rm n}(\epsilon) \sim |\epsilon|^{-\gamma}$ also leads to a negative contribution $m^2_{(2)} < -\frac{1}{4}$ that favors pairing. It is, by itself, always more negative than the AdS_2 Breitenlohner–Freedman (BF) bound $m^2_{\rm BF} = -\frac{1}{4}$ that signals the onset of instability in AdS space[53–56]. The zero-temperature phase transition takes place when $m^2 = m^2_{(1)} + m^2_{(2)}$ equals $m^2_{\rm BF}$. This holographic condition is indeed identical to the one obtained from the Eliashberg equation[45].

The holographic map was established at zero temperature. Since the normal state SYK physics in the IR is controlled by a conformal fixed point, the finite-T theory at Euclidean time is mathematically directly related to the zero temperature one[51]. The same is true in the AdS_2 theory: the black hole geometry is equivalent to the $T = 0$ background after a coordinate transformation[57,58]. Tracing the transformation, the SYK model precisely translates to the finite T version of the action (5) but with the space-time metric of a Euclidean AdS_2 black hole

$$ds^2 = \frac{1}{\zeta^2}\left((1-\zeta^2/\zeta_T^2)d\tau^2 + \frac{1}{(1-\zeta^2/\zeta_T^2)}d\zeta^2\right). \quad (7)$$

$\zeta_T^{-1} = 2\pi T$ encodes the location of the black hole horizon, see Methods section.

Finally, we comment on the holographic map at finite chemical potential μ. At low energies, the normal state SYK model possesses an emergent U(1) symmetry[51]. It allows to relate the normal state fermion propagator at finite μ to the one for $\mu = 0$. For $\Pi_{\rm n}(\omega,\epsilon)$ this amounts to the shift $\omega \to \omega - i4\pi q\mathcal{E}T$. On the other hand, the propagator of a charge q^* scalar particle within AdS_2 that is exposed to a boundary electric field E, yields an analogous shift $\omega \to \omega - i2\pi q^* ET$[59]. Hence, the holographic boundary electric field $E = \mathcal{E}$ is given by the spectral asymmetry of the SYK model with effective charge $q^* = 2q$ of the Cooper pair. Within the gauge $A_\zeta = 0$ this yields the vector potential $A_\tau = \frac{i\mathcal{E}}{\zeta}(1-\zeta/\zeta_T)$. Our results are summarized in Table 1.

Pairing response

Though we have equated the actions, this only implies that the dynamical equations of motions match. For a true equivalent mapping, the response to an external source field must also

Table 1. Dictionary of the Eliashberg-gravity map. Summary of the correspondence between the degrees of freedom of the critical Eliashberg-SYK theory and those of (1+1)-dimensional holographic superconductor. Notice ζ and τ are related to $1/\epsilon$ and the absolute time by a Radon transformation.

Field-theory side	Gravity side
frequency ϵ of time lag $\tau_1 - \tau_2$	holographic dimension ζ
absolute time $(\tau_1 + \tau_2)/2$	time (Euclidean) τ
anomalous propagator F	order parameter field ψ
fermion bubble $\Pi_n(\omega, \epsilon)$	$\partial_\tau\psi$, mass contrib. $m^2_{(1)} > 0$
pairing interaction $D_n(\epsilon)$	$\partial_\zeta\psi$, mass contrib. $m^2_{(2)} < 0$
Cooper pair charge $2q$	condensate charge $q_\star$
spectral asymmetry $\mathcal{E}$	AdS_2 electric field E

correspond. We can do so by checking an explicit observable, the order parameter susceptibility in the normal phase.

We add an external pairing field $J_0(\tau)$ to the action:

$$S_J = -\int d\tau J_0(\tau) \sum_i c_{i\uparrow}(\tau) c_{i\downarrow}(\tau) + \text{h.c.}. \tag{8}$$

$J_0(\tau)$ is conjugate to the dynamic order parameter $\mathcal{O}(\tau) = \lim_{\tau' \to \tau} \langle F(\tau, \tau') \rangle$ and physically realizable via coupling through a Josephson junction. Using our holographic map this yields in the gravitational formulation $S_J = -\int d^2x \sqrt{g}(J(x)\psi^*(x) + \text{h.c.})$ where at low frequencies $J(\tau, \zeta) = \frac{c}{c_0} \zeta^{\frac{1-\gamma}{2}} J_0(\tau)$. The corresponding Euler–Lagrange equation is the inhomogeneous Klein–Gordon equation in AdS_2:

$$\partial_\zeta^2 \psi + V(\omega, \zeta)\psi = \frac{J(\omega, \zeta)}{\zeta^2}, \tag{9}$$

with potential $V(\omega, \zeta) = -\frac{m^2}{\zeta^2} + (i\omega + 2q\mathcal{E}/\zeta)^2$. It appears the source term is present in the AdS-bulk, in contrast to the usual holographic reasoning, where one only expects effects of a source on the boundary, i.e., in the limit of small ζ dual to the UV. To address this issue, let us first consider static solutions $\omega = 0$. If we shift $\psi(0, \zeta) \to \psi(0, \zeta) + J(0, \zeta)/(\nu^2 - \frac{1}{4}\gamma^2)$ with constant

$$\nu^2 = \frac{1}{4} + m^2 - (2q\mathcal{E})^2, \tag{10}$$

the l.h.s. of (9) is unchanged but the source disappears from the r.h.s., i.e., from the bulk. It only enters through the UV boundary condition; see below. Thus, the new variable ψ can be understood as a combination of a boundary-sourced field and a source. This is in full accordance with holographic AdS/CFT where the same dynamical variable describes both the source (its boundary value) and the response. Eliashberg's theory is in practice always considered at $\omega = 0$. Further below we, therefore, follow holography to generalize this to finite ω by using double-trace deformations.

The Euler–Lagrange Eq. (9) should be identical to the stationary Eliashberg equation that follows from the original formulation of SYK model Eq. (3). Expressed in terms of the anomalous self energy $\Phi(\epsilon) = F(0, \epsilon)/\Pi_n(0, \epsilon)$, the stationary equation for F becomes

$$\Phi(\epsilon) = \lambda_p \bar{\mu}_\gamma \int_{\epsilon'} \frac{\Phi(\epsilon')}{|\epsilon - \epsilon'|^\gamma |\epsilon'|^{1-\gamma}} + J_0, \tag{11}$$

with time-independent source J_0 and $\bar{\mu}_\gamma = \mu_\gamma \Gamma(\gamma)\Gamma^2\left(\frac{1-\gamma}{2}\right)\left(2\cos\frac{\pi\gamma}{2} - \sin(\pi\gamma)\right)$. This equation is identical to the linearized gap equation of the Eliashberg theory of numerous finite-dimensional compressible quantum-critical metals[10–12]. Thus, our analysis goes beyond the specifics of the SYK model and is directly relevant to a much broader class of physical systems. The power-law behavior in Eq. (11) holds only within an upper (UV) and lower (IR) cut-off Λ and T, respectively. The relationship between (11) and Eq. (9) is particularly transparent in the limit of small γ, where, using $\tilde{\Phi} \equiv \Phi - J_0$, the former takes the form of a differential equation $\partial_\epsilon \epsilon^{1-\gamma} \partial_\epsilon \epsilon^\gamma \tilde{\Phi}(\epsilon) = -\gamma \lambda_p \bar{\mu}_\gamma \frac{\tilde{\Phi}(\epsilon) + J_0}{\pi\epsilon}$ with UV and IR boundary conditions $\partial_\epsilon \epsilon^\gamma \tilde{\Phi}(\epsilon)_{\epsilon=\Lambda} = \partial_\epsilon \tilde{\Phi}(\epsilon)_{\epsilon=T} = 0$[12,19,45]. With our holographic map, we rewrite this in terms of $\psi(\zeta) \propto \zeta^{\frac{1-\gamma}{2}} \tilde{\Phi}(c/\zeta)$, which precisely reproduce the Euler–Lagrange equation (9) for vanishing ω and $\mathcal{E}$ and with correct source $J(\zeta) \propto \zeta^{\frac{1-\gamma}{2}} J_0$. If we now analyse Φ, instead of $\tilde{\Phi}$, this is the equivalent of the earlier shift of ψ by the source. Then J_0 disappears from the bulk and only enters through the UV boundary condition: $\partial_\epsilon \epsilon^\gamma \Phi(\epsilon)_{\epsilon=\Lambda} = \gamma \Lambda^{\gamma-1} J_0$, as expected.

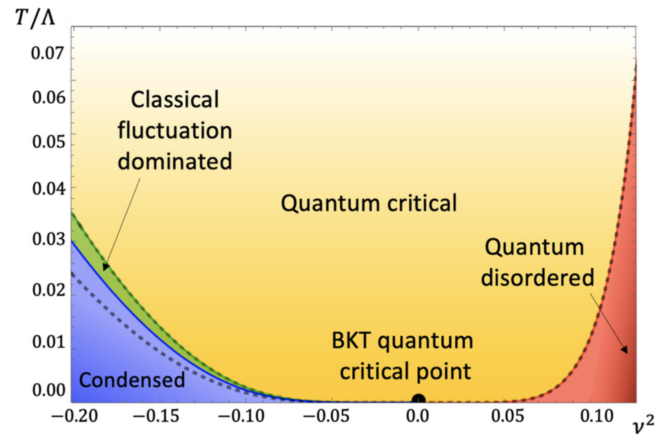

Fig. 2 Phase diagram of the SYK model. Phase diagram as a function of temperature T and ν^2 defined in Eq. (10) with $\gamma = 0.9$. The susceptibility diverges at the transition temperature T_c (solid line) that vanishes in a BKT-like fashion at $\nu^2 = 0$. Below T_c we have superconducting order (blue). Between the dashed lines we find classical critical behavior with Curie–Weiss susceptibility and critical slowing down $\chi \sim t_{\text{dyn}} \sim (T - T_c)^{-1}$ (we only calculated the upper dashed curve, the lower one is an educated guess). As the susceptibility is finite at the BKT quantum critical point, quantum criticality is identified by the regime where $\partial_T \chi(T) \sim 1/(T \log^2 T)$ (yellow region). In the quantum-disordered region (red) $\partial_T \chi(T)$ saturates as $T \to 0$. The quantum critical and quantum-disordered regimes are separated by a crossover.

The $\omega = 0$ solution of the homogeneous version of Eq. (9), i.e., for the shifted field, is

$$\psi(0, \zeta) = A\zeta^{\frac{1}{2} - \nu} + B\zeta^{\frac{1}{2} + \nu}, \tag{12}$$

where A and B are determined by the boundary condition translated for $\psi(\omega, \zeta)$, where ν^2 of (10) is a convenient measure of the mass and charge that vanishes at the BF bound.

We can now easily determine the static susceptibility. Written with an eye on the holographic computations, it reads

$$\chi = \left.\frac{d\mathcal{O}}{dJ_0}\right|_{J_0 = 0} = \chi_c \frac{b_+ + b_- \mathcal{G}(T)\Lambda^{-2\nu}}{a_+ + a_- \mathcal{G}(T)\Lambda^{-2\nu}}, \tag{13}$$

where $\mathcal{G}(T) = c^{2\nu}\frac{B}{A} = \frac{2\nu - \gamma}{2\nu + \gamma} T^{2\nu}$ with c from (4) contains the dependence on the IR behavior, while $a_\pm = b_\pm (1 \pm 2\nu/\gamma)^2$ and $b_\pm = 1 \mp 2\nu/\gamma$ as well as $\chi_c = 2c_g^2 \Lambda^\gamma / (\pi\gamma)$.

The static susceptibility determines the phase diagram of the model shown in Fig. 2. The regime with superconducting order corresponds to ν being imaginary. In that case, there are solutions for the order parameter obeying the source-less $J_0 = 0$ boundary conditions. This occurs whenever the denominator in Eq. (13) vanishes which determines the superconducting transition

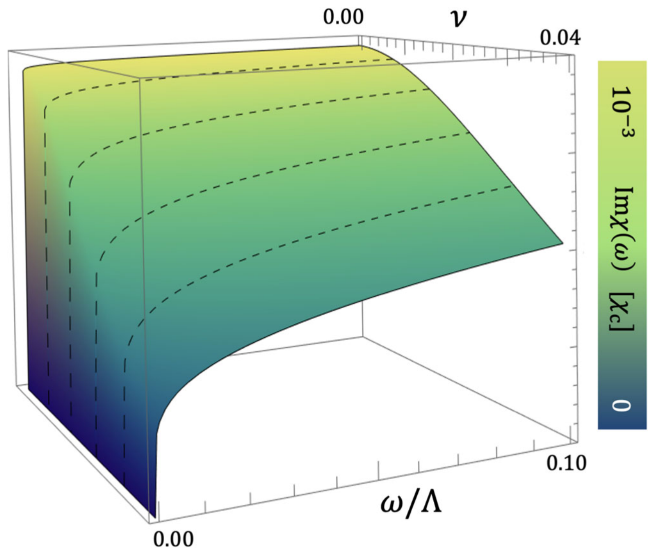

Fig. 3 Dynamical susceptibility away from criticality. Imaginary part of the dynamic pairing susceptibility $\chi(\omega)$ for different values of the pair breaking, parametrized in terms of ν with $\gamma = 0.01$ and $T/\Lambda = 10^{-4}$. Notice the broad continuum right at the BKT quantum critical point that only decays like $1/\log^2\omega$ at lowest frequencies.

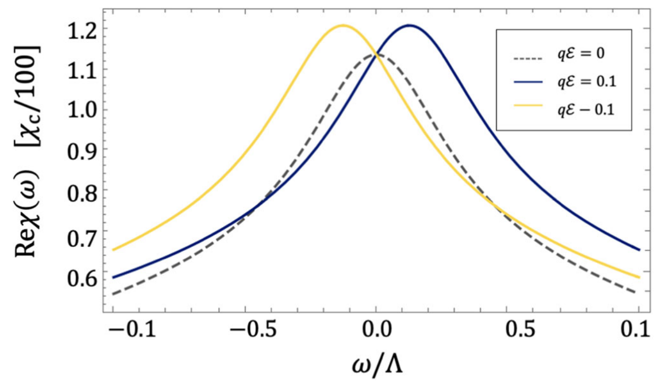

Fig. 4 Dynamical susceptibility away from charge neutrality. Real part of the dynamic pairing susceptibility $\chi(\omega)$ for different values of boundary electric fields $\mathcal{E}$ corresponding to different carrier density with $\gamma = 0.01, \nu = 10^{-3}$, and $T/\Lambda = 10^{-2}$. Notice spectral asymmetry away from $n = 1/2$.

temperature:

$$T_c \sim \Lambda e^{-\frac{\pi}{\sqrt{-\nu^2}}}. \tag{14}$$

In Fig. 2 the ordered state is shown in blue. One recognizes a Berezinskii–Kosterlitz–Thouless (BKT) phase transition[60–62] at a critical value of the pair-breaking parameter λ_p that corresponds to $\nu = 0$. Right above T_c the susceptibility diverges according to the mean-field Curie–Weiss law $\chi(T) \sim (T - T_c)^{-1}$. This happens in the classical regime marked green in Fig. 2. Note that at the BKT quantum critical point the order parameter susceptibility is χ_c and stays finite. This is in apparent contradiction with the behavior at quantum phase transitions, where commonly, the order parameter response to the external field is divergent. However, the milder BKT quantum criticality is signaled by a diverging slope of the susceptibility as it approaches this finite value $\partial_T\chi(\nu = 0) \approx \frac{4\chi_c}{\gamma T \log^2(\Lambda/T)}$ and $\partial_{\nu^2}\chi(T = 0) \propto \chi_c/\nu$, fully consistent with results obtained from holography[63,64]. The regime in the phase diagram where this is the behavior for $\partial_T\chi$ is indicated in yellow in Fig. 2, while saturation of the slope happens below the crossover to the quantum-disordered regime (marked red).

Eq. (13) is purposely written to be recognized as identical to the susceptibility obtained from a holographic approach based on the crossover from a higher-dimensional holographic theory AdS_{d+2} at high energies to $AdS_2 \times \mathbb{R}^d$ at low energies[63,64]. Below we discuss how the effect of the higher-dimensional space can be incorporated via appropriated double-trace deformations directly in the AdS_2 model Eq. (5)[24,65]. This insight allows us to use the power of holography and determine the dynamic pairing susceptibility. Using the approach of refs. [63,64] we obtain $\chi(\omega)$ immediately from the static susceptibility of Eq. (13) if we replace $\mathcal{G}(T)$ by

$$\mathcal{G}(T,\omega) = \frac{2\nu - \gamma}{2\nu + \gamma} T^{2\nu} \frac{\Gamma(u-\nu)\Gamma(v+\nu)}{\Gamma(u+\nu)\Gamma(v-\nu)}, \tag{15}$$

with $u = \frac{1}{2} + i2q\mathcal{E}$ and $v = \frac{1}{2} - i\frac{\omega - 4\pi T q\mathcal{E}}{2\pi T}$. Here we use retarded functions, i.e. in-falling boundary conditions at the black hole horizon[59]. In Fig. 3 we show the resulting frequency dependence of the imaginary part of the pairing susceptibility at low T as a function of ω for varying ν. Most notable is the almost flat behavior right at the quantum critical point, where at lowest frequencies holds that $\mathrm{Im}\chi(\omega) \approx \frac{2\pi}{\gamma}\log^{-2}(\Lambda/\omega)$. This mirrors the temperature dependence discussed earlier. Near the classical transition at finite T_c, we obtain critical slowing down behavior $\mathrm{Im}\chi(\omega) \sim \frac{\omega t_{dyn}}{1+(\omega t_{dyn})^2}$ with order-parameter relaxation time $t_{dyn} \sim (T - T_c)^{-1}$. In Fig. 4 we also show the impact of a deviation of the charge density from half-filling, which induces a finite boundary electric field $\mathcal{E}$ and a spectral asymmetry of the two particle response.

Finally, we establish a more direct connection between the susceptibility of the SYK model and holography in AdS_2 without having to resort to a crossover argument from higher-dimensional gravitational spaces. To this end, we need to posit the correct holographic boundary conditions for AdS_2. In holography, boundary conditions at $\zeta = 0$ crucially encode the precise theory one describes beyond the physics of interest within that theory. For AdS_2 models, this is a more detailed exercise, as the UV does not decouple as it does in higher-dimensional theories[66], and further UV information is necessary to describe the theory. In brief: standard boundary conditions correspond to a theory where $A = \lim_{\zeta\to 0}\zeta^{\nu-\frac{1}{2}}\psi(\zeta) \equiv J_0$ with J_0 the external source conjugate to the operator of interest, and $B = \lim_{\zeta\to 0}\frac{\zeta^{1-2\nu}}{2\nu}\partial_\zeta\zeta^{\nu-\frac{1}{2}}\psi|_{\zeta=0} = \mathcal{O}$ as the response; alternative quantization boundary conditions correspond to $B = J_0$, $A = \mathcal{O}$; a dual theory with so-called double-trace deformations corresponds to mixed boundary conditions of the type $B = fA + J_0$, $B = \mathcal{O}$, where f is an arbitrary coupling constant, or in alternative quantization[24] $A = fB + J_0$, $A = \mathcal{O}$. When the UV does not decouple, however, there is a new, fourth possibility, where one includes the contribution of the leading UV operator. This corresponds to mixed boundary conditions $B = fA + J_0$ and a mixed response $B = gA + \mathcal{O}$ with again g an arbitrary constant. The susceptibility computed from AdS_2 is[59]

$$\chi_{AdS_2} = \frac{d}{dJ_0}\mathcal{O} \simeq \frac{\mathcal{O}}{J_0} = \frac{B - gA}{B - fA} = \frac{1 - g\mathcal{G}}{1 - f\mathcal{G}}. \tag{16}$$

Up to normalization, this equals the holographic result obtained via dimensional crossover[59] and the SYK susceptibility Eq. (13).

DISCUSSION

The low-energy theory of the SYK Hamiltonian Eq. (1) can thus be formulated in terms of the action

$$S = S_{gravity} + S_{sc} + S_J. \tag{17}$$

$S_{gravity}$ is the much-discussed AdS gravity in $1 + 1$ dimensions which eventually gives rise to the Schwarzian theory, describing the SYK normal state[35,36]. It determines the metric of Eqs. (6) and (7). Hence the non-Fermi liquid normal state provides the gravitational background. Superconducting degrees of freedom of the SYK model then behave like a charge $2q$ matter field on the AdS_2 background with:

$$S_{sc}=N\int d^2x\sqrt{g}\left(D_a\psi^*D^a\psi+m^2|\psi|^2\right), \tag{18}$$

where $D_a=\partial_a-i2qA_a$. The finite temperature theory is equivalent to a change of coordinates that corresponds to a black hole with an event horizon given by the Hawking temperature. Deviations of the density from half-filling give rise to a boundary electric field $\mathcal{E}$. The competition between suppressed pairing due to the absence of quasiparticles and the enhanced, singular pairing interaction is merely a balance of two contributions to the mass m and leads to a quantum critical point of the BKT variety. The Euler–Lagrange equation of the gravitational theory maps directly onto the Eliashberg equation intensely studied in the context of quantum critical metals. External fields that couple to Cooper pairs act on the AdS_2 boundary. We have therefore attained an explicit and complete AdS-field theory correspondence.

Our derivation of holographic superconductivity from a microscopic Hamiltonian allows for a deeper and more concrete understanding of the holographic principle. In its spirit it is somewhat analogous to the microscopic derivation of Ginzburg–Landau theory from the BCS model by Gork'ov[67]; the result may be obvious for symmetry reasons, but yields explicit expressions of the parameters of the theory while allowing for all the practical simplifications that come with the order-parameter field theory. Our approach should be the natural starting point to study superconducting fluctuations beyond the Eliashberg limit, nonlinear effects beyond the Gaussian mean-field level, for systems as diverse as magnetic and nematic quantum critical points, or critical spin liquids, and the thermodynamic contributions from the order parameter condensation. In the holographic language, those effects correspond to quantum gravity corrections and gravitational back reactions, respectively. Moreover, as these systems are experimentally probed[23,44], it provides a direct avenue to test holography in the lab.

METHODS

SYK action of bilocal fields

In what follows we analyze the action of the SYK superconductor that comes from the Hamiltonian Eq. (1). The distribution function of couplings $g_{ij,k}=g'_{ij,k}+\mathrm{i}g''_{ij,k}$ includes a parameter α which interpolates between the Gaussian unitary and orthogonal ensembles. Specifically

$$\begin{aligned}\overline{g'_{ij,k}g'_{i'j',k'}}&=\left(1-\tfrac{\alpha}{2}\right)\tfrac{\bar{g}^2}{2N^2}\delta_{kk'}\left(\delta_{ii'}\delta_{jj'}+\delta_{ij'}\delta_{ji'}\right),\\ \overline{g''_{ij,k}g''_{i'j',k'}}&=\alpha\tfrac{\bar{g}^2}{4N^2}\delta_{kk'}\left(\delta_{ii'}\delta_{jj'}-\delta_{ij'}\delta_{ji'}\right).\end{aligned} \tag{19}$$

$\alpha=0$ corresponds to time-reversal symmetric configurations, while for $\alpha=1$ time reversal is fully broken.

As is common practice in the theory of SYK-like models we use bilocal fields, i.e., collective field variables that depend on two time variables. The effective action of the superconducting Yukawa-SYK problem is[41,45]:

$$\begin{aligned}S=&-N\mathrm{tr}\log\left(\hat{g}^{-1}-\hat{\Sigma}\right)+\tfrac{M}{2}\mathrm{tr}\log\left(d^{-1}-\Pi\right)\\&-N\left(G\otimes\Sigma+\widetilde{G}\otimes\widetilde{\Sigma}+F\otimes\Phi+F^\dagger\otimes\Phi^\dagger\right)+\tfrac{M}{2}D\otimes\pi\\&-\tfrac{M}{2}\bar{g}^2\left((G\widetilde{G})\otimes D+(1-\alpha)\left(F^\dagger F\right)\otimes D\right),\end{aligned} \tag{20}$$

with M boson flavors and N fermion flavors. We use the notation $A\otimes B=\int d\tau_1d\tau_2A(\tau_1,\tau_2)B(\tau_2,\tau_1)$ as well as $F^\dagger(\tau_1,\tau_2)=F(\tau_2,\tau_1)^*$ and $\widetilde{G}(\tau_1,\tau_2)=-G(\tau_2,\tau_1)$. The fermionic self energy and propagator are matrices in Nambu space:

$$\hat{\Sigma}=\begin{pmatrix}\Sigma & \Phi\\ \Phi^\dagger & \widetilde{\Sigma}\end{pmatrix}\ \text{and}\ \hat{G}=\begin{pmatrix}G & F\\ F^\dagger & \widetilde{G}\end{pmatrix}. \tag{21}$$

The bare propagators are given as

$$\begin{aligned}\hat{g}^{-1}(\tau,\tau')=&\ -(\partial_\tau\hat{\sigma}_0-\mu\hat{\sigma}_z)\delta(\tau-\tau'),\\ d^{-1}(\tau,\tau')=&\ -\left(\partial_\tau^2-\omega_0^2\right)\delta(\tau-\tau'),\end{aligned} \tag{22}$$

where the $\hat{\sigma}_i$ are 2×2 Nambu-space matrices. For large N and M, but fixed N/M the exact solution of the single-particle problem is given in terms of the stationary condition $\delta S=0$, which is given by the Eliashberg equations:

$$\begin{aligned}\mathrm{i}\epsilon_n(1-Z(\epsilon_n))&=-\bar{g}^2\tfrac{M}{N}T\sum_{n'}\tfrac{D(\epsilon_n-\epsilon_{n'})\mathrm{i}\epsilon_{n'}Z(\epsilon_{n'})}{(\epsilon_{n'}Z(\epsilon_{n'}))^2+\Phi(\epsilon_{n'})^2},\\ \Phi(\epsilon_n)&=\bar{g}^2\lambda_pT\sum_{n'}\tfrac{D(\epsilon_n-\epsilon_{n'})\Phi(\epsilon_{n'})}{(\epsilon_{n'}Z(\epsilon_{n'}))^2+\Phi(\epsilon_{n'})^2}.\end{aligned} \tag{23}$$

Here, we considered $\mu=0$ and used $\hat{\Sigma}(\epsilon_n)=\mathrm{i}\epsilon_n(1-Z(\epsilon_n))\hat{\sigma}_z+\Phi(\epsilon_n)\hat{\sigma}_x$. This equation has to be supplemented by a corresponding expression for the boson self energy[41].

In the normal state, the expectation values of Φ and F vanish. Hence, near the superconducting transition, we can expand for small Φ and F. This yields

$$\begin{aligned}S^{(sc)}=&\ \Phi^\dagger\otimes G_n\otimes\Phi\otimes G_n-\tfrac{\bar{g}^2\lambda_p}{2}\left(F^\dagger F\right)\otimes D_n\\&-F^\dagger\otimes\Phi-F\otimes\Phi^\dagger,\end{aligned} \tag{24}$$

where G_n and D_n are the finite temperature propagators of the normal state. If we now use that G_n and D_n only depend on the time difference, Fourier transform to frequency space, and integrates over the Gaussian fields Φ and $\Phi^\dagger$ we obtain Eq. (3) of the main text.

The particle number n is related to the spectral asymmetry $\mathcal{E}$ through the generalized Luttinger theorem[49,50]:

$$n=\frac{1}{2}-\frac{\theta}{\pi}-\frac{1-\gamma}{4}\frac{\sin(2\theta)}{\cos(\pi\gamma/2)}, \tag{25}$$

where $\tan\theta=\tan\left(\frac{\pi(1+\gamma)}{4}\right)\tanh(\pi q\mathcal{E})$. In the main text, we give in Eq. (2) the normal state propagators as function of time. Fourier transformation yields

$$\begin{aligned}&G_n(\epsilon)=c_g(\tan\theta+\mathrm{i}\,\mathrm{sign}(\epsilon))|\epsilon|^{-\frac{1-\gamma}{2}},\\&D_n(\epsilon)=c_d|\epsilon|^{-\gamma},\end{aligned} \tag{26}$$

where the coefficients are

$$\begin{aligned}c_g&=2b_g\Gamma\left(\tfrac{1-\gamma}{2}\right)\cos\left(\tfrac{\pi}{4}(1+\gamma)\right),\\ c_d&=2b_d\Gamma(\gamma)\cos(\pi\gamma/2),\end{aligned} \tag{27}$$

and the exponent γ is determined by

$$\frac{(1-\gamma)\tan\frac{\pi(1+\gamma)}{4}}{1+\tan^2\frac{\pi(1+\gamma)}{4}\tanh^2(\pi q\mathcal{E})}=\frac{M}{N}\frac{\gamma\tan\frac{\pi\gamma}{2}}{1-\tanh^2(\pi q\mathcal{E})}. \tag{28}$$

Derivation of the holographic map at $T=\mu=0$

First, we summarize the derivation of Eqs. (4) and (5).

We expand in Eq. (3) the zero-temperature expression of $\Pi_n^{-1}(\omega,\epsilon)$ for small $\omega\ll\epsilon$ up to ω^2:

$$\frac{1}{\Pi_n(\omega,\epsilon)}\approx\frac{1}{c_g^2}|\epsilon|^{1-\gamma}\left(1-\frac{1-\gamma}{8}\left(\frac{\omega}{\epsilon}\right)^2\right). \tag{29}$$

Let us focus first focus on the $\omega=0$ limits of the above expression. The effective action is given by

$$\frac{S^{(sc)}}{c_g^{-2}N}=\int_{\omega,\epsilon\epsilon'}F^\dagger(\omega,\epsilon)\left(\frac{\delta(\epsilon-\epsilon')}{|\epsilon|^{\gamma-1}}-\frac{\hat{\mu}}{|\epsilon-\epsilon'|^\gamma}\right)F(\omega,\epsilon') \tag{30}$$

with $\hat{\mu}=c_d\bar{g}^2\lambda_pc_g^2/2$. To proceed we perform a Mellin transform

$$F(\omega,\epsilon)=\int_{-\infty}^{\infty}\frac{dw}{\sqrt{2\pi}}f_w(\omega)|\epsilon|^{iw-1+\gamma/2}. \tag{31}$$

The action then becomes a set of uncoupled oscillators:

$$\frac{S^{(sc)}}{c_g^{-2}N}=\int_\omega\frac{dw}{\pi}\left(1-\frac{\hat{\mu}}{2\pi}r_w\right)f_w^\star f_w, \tag{32}$$

where

$$\begin{aligned} r_w &= \int_{-\infty}^{\infty} dx \frac{|x|^{iw}}{|1-x|^{\gamma}|x|^{1-\gamma/2}} \\ &= \frac{\pi^2/2}{\Gamma(\gamma)\cos\left(\frac{\pi\gamma}{2}\right)\left|\sinh\left(\frac{\pi}{4}(2w-i\gamma)\right)\Gamma\left(1+iw-\frac{\gamma}{2}\right)\right|^2}. \end{aligned} \quad (33)$$

To proceed it is convenient to introduce $s = 2w/\gamma$ and use the field variable

$$g_s = \gamma\sqrt{\frac{r_{\frac{\gamma}{2}s}}{8}} f_{\frac{\gamma}{2}s}. \quad (34)$$

Then we obtain the action

$$\frac{S^{(sc)}}{c_g^{-2}N} = \int_\omega \frac{ds}{2\pi}\left(q_s - \frac{4\tilde{\mu}}{\pi\gamma}\right) g_s^* g_s, \quad (35)$$

where $q_s = 8/\gamma r_{\frac{\gamma}{2}s}$. Low energies correspond to small s, where we can expand

$$q_s = a_\gamma + b_\gamma s^2 + \mathcal{O}(s^4), \quad (36)$$

with positive coefficients

$$\begin{aligned} a_\gamma &= \frac{4\sin^2\left(\frac{\pi\gamma}{4}\right)\cos\left(\frac{\pi\gamma}{2}\right)\Gamma\left(-\frac{\gamma}{2}\right)^2\Gamma(\gamma+1)}{\pi^2}, \\ b_\gamma &= \frac{1}{16}\gamma^2\left(\pi^2\csc^2\left(\frac{\pi\gamma}{4}\right) - 4\psi^{(1)}\left(1-\frac{\gamma}{2}\right)\right)a_\gamma, \end{aligned} \quad (37)$$

with $\psi^{(1)}$ polygamma function. The coefficients a_γ and b_γ are of order 1 for small γ, whereas higher-order-in-$s$terms all vanish with increasing powers in γ. Therefore, the expansion Eq. (36) is correct for all values of the exponent γ if s is small, and for all s if γ is small. Hence at small γ it is not a low-energy expansion.

We now introduce

$$\tilde{\psi}(\omega, z) = c_\psi\sqrt{\frac{z}{2\pi}}\int ds g_s(\omega)\left|\frac{z}{c}\right|^{-i\frac{\gamma s}{2}}, \quad (38)$$

with $c_\psi = 2\sqrt{\frac{2}{r_0}}c^{\gamma/2-1}c_0$. From Eq. (35) it follows that

$$\frac{S^{(sc)}}{c_g^{-2}N} \approx \int_{z,\omega}\left(\frac{m^2}{z^2}|\tilde{\psi}|^2 + |\partial_z\tilde{\psi}|^2\right), \quad (39)$$

with squared mass given by

$$m^2 = m_{(1)}^2 + m_{(2)}^2. \quad (40)$$

Here $m_{(1)}^2 = \frac{\gamma^2 a_\gamma}{4b_\gamma} > 0$ and $m_{(2)}^2 = -\frac{\gamma\tilde{\mu}}{\pi b_\gamma} - \frac{1}{4}$. The implication is that with Eq. (34) the relationship between F and $\tilde{\psi}$ is non-local:

$$\tilde{\psi}(\omega, z) = c_\psi\sqrt{\frac{z}{8}}\int_\epsilon \mathcal{K}(z\epsilon)\frac{F(\omega,\epsilon)}{|\epsilon|^{\gamma/2}}, \quad (41)$$

with $\mathcal{K}(z\epsilon) = \int_w \sqrt{r_w}e^{-iw\log\left|\frac{z}{c}\epsilon\right|}$. However, at low energies $\mathcal{K}(z\epsilon) \propto \delta(z\epsilon - c)$ and it becomes local and yields the mapping Eq. (4).

We now include the finite-frequency part of Eq. (29) and Fourier transform from ω to Euclidean time t. One easily finds:

$$\frac{S^{(sc)}}{c_g^{-2}N} \approx \int_{z,t}\left(\frac{m^2}{z^2}|\tilde{\psi}|^2 + |\partial_z\tilde{\psi}|^2 - |\partial_t\tilde{\psi}|^2\right). \quad (42)$$

Finally, the two coefficients in Eq. (4) are

$$c_0^2 = \frac{b_\gamma r_0 c^{\gamma-2}}{2\gamma^2 c_g^2}, \quad (43)$$

$$c^{2(\gamma-1)} = \frac{(1-\gamma)\gamma^2}{4\pi b_\gamma r_0}. \quad (44)$$

This completes the derivation of the action in Lorentzian de Sitter space with mass $m^2 = m_{(1)}^2 + m_{(2)}^2$.

To transform the problem to AdS_2 we follow ref. [52] and use the Radon transform which takes the explicit form

$$\begin{aligned} \tilde{\psi}(z,t) = \ & (\mathcal{R}\psi)(z,t) = 2z\int_{t-z}^{t+z} d\tau \int_0^\infty \frac{d\zeta}{\zeta}\psi(\zeta,\tau) \\ & \times \delta\left(z^2 - (\tau-t)^2 - \zeta^2\right). \end{aligned} \quad (45)$$

If one now uses that one can relate the Laplacian before and after the Radon transformation $\square_{dS_2}\mathcal{R}\psi = -\mathcal{R}(\square_{AdS_2}\psi)$ it follows that the Radon transform $\tilde{\eta}_\lambda = \mathcal{R}\eta_\lambda$ of an eigenfunction η_λ of the Laplacian in AdS_2 is also an eigenfunction of $\square_{dS_2}$. It is however not normalized. Addressing this issue through so-called leg factors[52] one obtains at low energy the action (5) in AdS_2 with modified mass

$$\overline{m}^2 = m_{BF}^2 + \frac{m^2 - m_{BF}^2}{\left[1 - 4G\left(m^2 - m_{BF}^2\right)\right]}. \quad (46)$$

$G = \sum_{n=0}^\infty \frac{(-1)^n}{(2n+1)^2} \approx 0.915966$ is Catalan's constant. Near the Breitenlohner–Freedman bound $m_{BF}^2 = \frac{1}{4}$ both masses are the same, which is the reason why we did not distinguish between m and $\overline{m}$ in the main text. This completes the holographic map.

If we specify the density n, the ratio of boson and fermion flavors M/N, and the pair-breaking strength α the three crucial quantities $\mathcal{E}$, γ and λ_p are fixed and the gravitational theory is well defined. Only one number - in our case b_g —has to be fixed from a numerical solution of the SYK model. However it only determines the global factor c_0 of the holographic action.

Holographic map at finite temperatures

In the analysis at finite temperatures, we start from the action for the SYK-superconductor Eq. (24) without integrating out the conjugate field $\Phi(\tau_1, \tau_2)$. We have to keep in mind that the time integrations go from $-\beta/2$ to $\beta/2$ where $\beta = 1/T$. Similarly, G_n and D_n are the finite temperature propagators of the normal state. Using the invariance of the low-energy saddle point equations under re-parametrization $\tau \to \overline{\tau} = f(\tau)$, both functions can be obtained from the $T = 0$ solutions $G_{n,0}(\tau)$ and $D_{n,0}(\tau)$ via

$$\begin{aligned} G_n(\tau,\tau') &= f'(\tau)^{\frac{1+\gamma}{4}} G_{n,0}(f(\tau) - f(\tau')) f'(\tau')^{\frac{1+\gamma}{4}}, \\ D_n(\tau,\tau') &= f'(\tau)^{\frac{1-\gamma}{2}} D_{n,0}(f(\tau) - f(\tau')) f'(\tau')^{\frac{1-\gamma}{2}}, \end{aligned}$$

with $f(\tau) = \frac{\beta}{\pi}\tan\left(\frac{\pi\tau}{\beta}\right)$. Hence, the finite temperature problem leads to effective action, identical to the one we analyzed at $T = 0$, yet in terms of the field

$$\begin{aligned} \overline{F}(\overline{\tau}_1, \overline{\tau}_2) = \ & \left(1 + (\pi T)^2\overline{\tau}_1^2\right)^{-\frac{1+\gamma}{4}}\left(1 + (\pi T)^2\overline{\tau}_2^2\right)^{-\frac{1+\gamma}{4}} \\ & \times F\left(f^{-1}(\overline{\tau}_1), f^{-1}(\overline{\tau}_2)\right) \end{aligned} \quad (47)$$

Hence, we can immediately make the identification that is analogous to Eq. (4) only in terms of the new function $\overline{F}$ instead of F and with transformed variable $\overline{\tau}_{1,2}$ instead of $\tau_{1,2}$. The scalar field, expressed in terms of the anomalous propagator field, that replaces (4) at finite temperatures is then:

$$\tilde{\psi}(\overline{t}, \overline{z}) = c_0|\overline{z}|^{\frac{1-\gamma}{2}}\int_{-\infty}^\infty ds\overline{F}(t_+, t_-)e^{ics/\overline{z}}, \quad (48)$$

where $t_\pm = \overline{t} \pm \frac{s}{2}$. After performing an inverse Radon transformation from $\tilde{\psi}(\overline{t}, \overline{z})$ to $\psi(\overline{\tau}, \overline{\zeta})$, the holographic action can now be transformed from coordinates $(\overline{\tau}, \overline{\zeta})$ to (τ, ζ), where $0 < \tau < 1/T$, which agrees at the boundary with the original imaginary variables of the SYK model[58]

$$\begin{aligned} \overline{\tau} &= 2\zeta_T\frac{\left(1-\zeta^2/\zeta_T^2\right)^{1/2}\sin(\tau/\zeta_T)}{1+\left(1-\zeta^2/\zeta_T^2\right)^{1/2}\cos(\tau/\zeta_T)}, \\ \overline{\zeta} &= \frac{2\zeta}{1+\left(1-\zeta^2/\zeta_T^2\right)^{1/2}\cos(\tau/\zeta_T)}. \end{aligned} \quad (49)$$

where $\zeta_T = \frac{1}{2\pi T}$. In these coordinates the finite-T action of the SYK superconductor becomes

$$S^{(sc)}/N = \int_0^{\zeta_T} d\zeta\int_{-\beta/2}^{\beta/2} d\tau\left(\frac{m^2}{\zeta^2}\psi^*\psi + \frac{\partial_\tau\psi^*\partial_\tau\psi}{1-\zeta^2/\zeta_T^2} + \left(1-\zeta^2/\zeta_T^2\right)\partial_\zeta\psi^*\partial_\zeta\psi\right), \quad (50)$$

which is the correct finite-T version of a holographic superconductor in AdS_2 with black hole horizon ζ_T and metric Eq. (7).

DATA AVAILABILITY

The data that support the findings of this study are available from the authors on request.

Received: 9 December 2021; Accepted: 6 April 2022;
Published online: 01 June 2022

REFERENCES

1. Eliashberg, G. M. Interactions between electrons and lattice vibrations in a superconductor. *Sov. Phys. JETP* **11**, 696–702 (1960).
2. Eliashberg, G. M. Temperature Green's functions for electrons in a superconductor. *Sov. Phys. JETP* **12**, 1000–1002 (1961).
3. Migdal, A. B. Interaction between electrons and lattice vibrations in a normal metal. *Sov. Phys. JETP* **7**, 996–1001 (1958).
4. Mathur, N. D. et al. Magnetically mediated superconductivity in heavy fermion compounds. *Nature* **394**, 39–43 (1998).
5. Kasahara, S. et al. Evolution from non-Fermi to Fermi-liquid transport via isovalent doping in $BaFe_2(As_{1-x}P_x)_2$ superconductors. *Phys. Rev. B* **81**, 184519 (2010).
6. Sachdev, S. & Keimer, B. Quantum criticality. *Phys. Today* **64**, 29–35 (2011).
7. Balatsky, A. V. Superconducting instability in a non-Fermi liquid scaling approach. *Philos. Mag. Lett.* **68**, 251–256 (1993).
8. Sudbø, A. Pair susceptibilities and gap equations in non-Fermi liquids. *Phys. Rev. B* **74**, 2575–2578 (1995).
9. Yin, L. & Chakravarty, S. Spectral anomaly and high temperature superconductors. *Int. J. Mod. Phys. B* **10**, 805–845 (1996).
10. Abanov, A., Chubukov, A. & Finkel'stein, A. Coherent vs. incoherent pairing in 2D systems near magnetic instability. *Europhys. Lett.* **54**, 488–494 (2001).
11. Abanov, A., Chubukov, A. V. & Schmalian, J. Quantum-critical superconductivity in underdoped cuprates. *Europhys. Lett.* **55**, 369–375 (2001).
12. Chubukov, A. V. & Schmalian, J. Superconductivity due to massless boson exchange in the strong-coupling limit. *Phys. Rev. B* **72**, 174520 (2005).
13. She, J.-H. & Zaanen, J. BCS superconductivity in quantum critical metals. *Phys. Rev. B* **80**, 184518 (2009).
14. Abanov, A. & Chubukov, A. V. Interplay between superconductivity and non-Fermi liquid at a quantum critical point in a metal. I. The γ-model and its phase diagram at $T = 0$: the case $0 < \gamma < 1$. *Phys. Rev. B* **102**, 024524 (2020).
15. Wu, Y.-M., Abanov, A. & Chubukov, A. V. Interplay between superconductivity and non-Fermi liquid at a quantum critical point in a metal. II. The γ-model at finite T for $0 < \gamma < 1$. *Phys. Rev. B* **102**, 024525 (2020).
16. She, J.-H. et al. Observing the origin of superconductivity in quantum critical metals. *Phys. Rev. B* **84**, 144527 (2011).
17. Bonesteel, N. E., McDonald, I. A. & Nayak, C. Gauge fields and pairing in double-layer composite fermion metals. *Phys. Rev. Lett.* **77**, 3009–3012 (1996).
18. Metlitski, M. A., Mross, D. F. & Sachdev, S. Cooper pairing in non-Fermi liquids. *Phys. Rev. B* **91**, 115111 (2015).
19. Son, D. T. Superconductivity by long-range color magnetic interaction in high-density quark matter. *Phys. Rev. D.* **59**, 094019 (1999).
20. Roussev, R. & Millis, A. J. Quantum critical effects on transition temperature of magnetically mediated p-wave superconductivity. *Phys. Rev. B* **63**, 140504(R) (2001).
21. Raghu, S., Torroba, G. & Wang, H. Metallic quantum critical points with finite BCS couplings. *Phys. Rev. B* **92**, 205104 (2015).
22. Chowdhury, D. & Berg, E. The unreasonable effectiveness of Eliashberg theory for pairing of non-Fermi liquids. *Ann. Phys.* **417**, 168125 (2020).
23. Chubukov, A. V., Abanov, A., Esterlis, I. & Kivelson, S. A. Eliashberg theory of phonon-mediated superconductivity - when it is valid and how it breaks down. *Ann. Phys.* **417**, 168190 (2020).
24. Zaanen, J., Liu, Y., Sun, Y.-W. & Schalm, K. *Holographic Duality in Condensed Matter Physics* (Cambdrige Univ. Press, 2015).
25. Ammon, M. & Erdmenger, J. *Gauge/Gravity Duality: Foundations and Applications* (Cambridge Univ. Press, 2015).
26. Hartnoll, S. A., Lucas, A. & Sachdev, S. *Holographic Quantum Matter* (The MIT Press, 2018).
27. Hartnoll, S. A., Herzog, C. P. & Horowitz, G. T. Building a holographic superconductor. *Phys. Rev. Lett.* **101**, 031601 (2008).
28. Gubser, S. S. Breaking an Abelian gauge symmetry near a black hole horizon. *Phys. Rev. D.* **78**, 065034 (2008).
29. Maldacena, J. M. The large N limit of superconformal field theories and supergravity. *Adv. Theor. Math. Phys.* **2**, 231–252 (1998).
30. Sachdev, S. & Ye, J. Gapless spin liquid ground state in a random, quantum Heisenberg magnet. *Phys. Rev. Lett.* **70**, 3339–3342 (1993).
31. Sachdev, S. Holographic metals and the fractionalized Fermi liquid. *Phys. Rev. Lett.* **105**, 151602 (2010).
32. Chowdhury, D., Georges, A., Parcollet, O. & Sachdev, S. Sachdev-Ye-Kitaev models and beyond: a window into non-fermi liquids. Preprint at https://arxiv.org/abs/2109.05037 (2021).
33. Jian, S. K., Xian, Z. Y. & Yao, H. Quantum criticality and duality in the Sachdev-Ye-Kitaev/AdS_2 chain. *Phys. Rev. B* **97**, 205141 (2018).
34. Esterlis, I., Guo, H., Patel, A. A. & Sachdev, S. Large-N theory of critical Fermi surfaces. *Phys. Rev. B* **103**, 235129 (2021).
35. Maldacena, J. M. & Stanford, D. Remarks on the Sachdev-Ye-Kitaev model. *Phys. Rev. D.* **94**, 106002 (2016).
36. Maldacena, J. M., Stanford, D. & Yang, Z. Conformal symmetry and its breaking in two dimensional nearly anti-de-sitter space. *PTEP* **2016**, 12C104 (2016).
37. Bagrets, D., Altland, A. & Kamenev, A. Sachdev-Ye-Kitaev model as Liouville quantum mechanics. *Nucl. Phys. B.* **911**, 191–205 (2016).
38. Bagrets, D., Altland, A. & Kamenev, A. Power-law out of time order correlation functions in the SYK model. *Nucl. Phys. B.* **921**, 727–752 (2017).
39. Milekhin, A. Coupled Sachdev-Ye-Kitaev models without schwartzian dominance. Preprint at https://arxiv.org/abs/2102.06651 (2021).
40. Myers, R. C., Sierens, T. & Witczak-Krempa, W. A holographic model for quantum critical responses. *J. High. Energy Phys.* **1605**, 073 (2016).
41. Esterlis, I. & Schmalian, J. Cooper pairing of incoherent electrons: an electron-phonon version of the Sachdev-Ye-Kitaev model. *Phys. Rev. B* **100**, 115132 (2019).
42. Patel, A. A., Lawler, M. J. & Kim, E.-A. Coherent superconductivity with a large gap ratio from incoherent metals. *Phys. Rev. Lett.* **121**, 187001 (2018).
43. Wang, Y. Solvable strong-coupling quantum dot model with a non-Fermi-liquid pairing transition. *Phys. Rev. Lett.* **124**, 017002 (2020).
44. Chowdhury, D. & Berg, E. Intrinsic superconducting instabilities of a solvable model for an incoherent metal. *Phys. Rev. Res.* **2**, 013301 (2020).
45. Hauck, D., Klug, M. J., Esterlis, I. & Schmalian, J. Eliashberg equations for an electron–phonon version of the Sachdev–Ye–Kitaev model: pair breaking in non-Fermi liquid superconductors. *Ann. Phys.* **417**, 168120 (2020).
46. Gnezdilov, N. V. Gapless odd-frequency superconductivity induced by the Sachdev-Ye-Kitaev model. *Phys. Rev. B* **99**, 024506 (2019).
47. Klebanov, I. R., Milekhin, A., Tarnopolsky, G. & Zhao, W. Spontaneous breaking of U(1) symmetry in coupled complex SYK models. *J. High. Energy Phys.* **2011**, 162 (2020).
48. Nambu, Y. Quasi-particles and gauge invariance in the theory of superconductivity. *Phys. Rev.* **117**, 648 (1960).
49. Georges, A., Parcollet, O. & Sachdev, S. Quantum fluctuations of a nearly critical Heisenberg spin glass. *Phys. Rev. B* **63**, 134406 (2001).
50. Wang, Y. & Chubukov, A. V. Quantum phase transition in the Yukawa-SYK model. *Phys. Rev. Res.* **2**, 033084 (2020).
51. Sachdev, S. Bekenstein-Hawking entropy and strange metals. *Phys. Rev. X* **5**, 041025 (2015).
52. Das, R., Ghosh, A., Jevicki, A. & Suzuki, K. Space-time in the SYK model. *J. High. Energy Phys.* **1807**, 184 (2018).
53. Breitenlohner, P. & Freedman, D. Z. Stability in gauged extended supergravity. *Ann. Phys.* **144**, 249–281 (1982).
54. Hartnoll, S. A., Herzog, C. P. & Horowitz, G. T. Holographic superconductors. *J. High. Energy Phys.* **0812**, 015 (2008).
55. Gubser, S. S. & Nellore, A. Low-temperature behavior of the Abelian Higgs model in anti-de Sitter space. *J. High. Energy Phys.* **0904**, 008 (2009).
56. Denef, F. & Hartnoll, S. A. Landscape of superconducting membranes. *Phys. Rev. D.* **79**, 126008 (2009).
57. Faulkner, T., Iqbal, N., Liu, H., McGreevy, J. & Vegh, D. Holographic non-Fermi-liquid fixed points. *Philos. Trans. R. Soc. A* **369**, 1640–1669 (2011).
58. Sachdev, S. Universal low temperature theory of charged black holes with AdS_2 horizons. *J. Math. Phys.* **60**, 052303 (2019).
59. Faulkner, T., Liu, H., McGreevy, J. & Vegh, D. Emergent quantum criticality, Fermi surfaces, and AdS_2. *Phys. Rev. D.* **83**, 125002 (2011).
60. Kaplan, D. B., Lee, J.-W., Son, D. T. & Stephanov, M. A. Conformality lost. *Phys. Rev. D.* **80**, 125005 (2009).
61. Berezinskii, V. L. Destruction of long range order in one-dimensional and two-dimensional systems having a continuous symmetry group. I. Classical systems. *Sov. Phys. JETP* **32**, 493–500 (1971).
62. Kosterlitz, J. M. & Thouless, J. D. Ordering, metastability and phase transitions in two-dimensional systems. *J. Phys. Condens. Matter* **6**, 1181–1203 (1973).
63. Iqbal, N., Liu, H. & Mezei, M. Quantum phase transitions in semilocal quantum liquids. *Phys. Rev. D.* **91**, 025024 (2015).
64. Jensen, K. Semi-holographic quantum criticality. *Phys. Rev. Lett.* **107**, 231601 (2011).
65. Witten, E. Multi-trace operators, boundary conditions, and ads/cft correspondence. Preprint at https://arxiv.org/abs/hep-th/0112258 (2014).
66. Maldacena, J. M., Michelson, J. & Strominger, A. Anti-de sitter fragmentation. *J. High. Energy Phys.* **9902**, 011 (1999).
67. Gorkov, L. P. Microscopic derivation of the Ginzburg-Landau equations in the theory of superconductivity. *Sov. Phys. JETP* **9**, 1364–1367 (1959).

ACKNOWLEDGEMENTS

We are grateful to A.V. Chubukov and S. Hartnoll for helpful discussions. This research was supported in part by the Netherlands Organization for Scientific Research/Ministry of Science and Education (NWO/OCW), and the Deutsche Forschungsgemeinschaft (DFG, German Research Foundation)—TRR 288 - 422213477 Elasto-Q-Mat (project A07). We acknowledge support from the KIT-Publication Fund of the Karlsruhe Institute of Technology.

AUTHOR CONTRIBUTIONS

K.S. and J.S. conceived of the presented idea. All authors developed the theory. G.-A.I. performed the calculations and designed the figures. All authors discussed the results and contributed to the final manuscript.

FUNDING

Open Access funding enabled and organized by Projekt DEAL.

COMPETING INTERESTS

The authors declare no competing interests.

ADDITIONAL INFORMATION

Correspondence and requests for materials should be addressed to Gian-Andrea Inkof, Koenraad Schalm or Jörg Schmalian.

Reprints and permission information is available at http://www.nature.com/reprints

Publisher's note Springer Nature remains neutral with regard to jurisdictional claims in published maps and institutional affiliations.